Are 3D heat transfer formulations with short time sted and sun patch evolution nececessary for building simulation?

Auline Rodler, Jean-Jacques Roux, Joseph Virgone, E.J. Kim, Jean-Luc Hubert

ARE 3D HEAT TRANSFER FORMULATIONS WITH SHORT TIME STEP AND SUN PATCH EVOLUTION NECESSARY FOR BUILDING SIMULATION?

Rodler A.[1], Roux J-J.[1], Virgone J.[1], Eui-Jong K.[1], Hubert J-L.[2]
[1]CETHIL, UMR5008, CNRS, INSA-Lyon, Université Lyon 1, 20 Av A. Einstein, 69621 Villeurbanne Cedex, France
[2]Site EDF R&D des Renardières, Avenue des Renardières – Ecuelles, 77818 Moret-sur-Loing Cedex, France

ABSTRACT

A numerical model is developed to accurately simulate the transient thermal behaviour of rooms with sun-facing windows, with the use of a refined spatial and temporal discretization. For each node, the energy balance equations are developed based on a consideration of radiation, convection, air enthalpy and three-dimensional heat conduction. As buildings are exposed to rapid climatic variations (particularly incident solar radiation), we have added the different environmental conditions at short time-steps. The simulation considers the projection of solar radiation through a window onto interior walls, referred to as a sun patch. Therefore conduction transfer is treated in three dimensions. The indoor air temperature, the temperature of the cells in the walls and the surface temperatures are calculated at each time step using a variable-step Ordinary Differential Equation (ODE) solver.
Results from this model are compared to well-known simulation tools using one-dimensional heat conduction without a sun patch.

INTRODUCTION

In France, the residential sector represents 42 % of energy consumption (ADEME, 2005). The French building code is guiding the construction sector to embrace low energy building practices. This regulation imposes limitations on maximal primary energy consumption, the use of the energy systems, and upper limits on air infiltration. In order to comply with these standards, low-energy buildings may incorporate high levels of insulation, heat recovery systems and passive solar building design techniques.

As low energy buildings are generally well insulated, overheating of rooms can be a serious issue. Therefore, it is important to assess the performance of current transient thermal models when adapted to low energy buildings, defined as those with particularly thick and insulated walls. Contemporary thermal models, like TrnSys (TRNSYS Mathematical Reference, 1996), Dymola (Dymola Version 2013) and Codyba (www.jnlog.com/codyba1.htm) are typically used to predict performance over the course of a year. As a result, certain features of heat transfer in building envelopes are simplified or neglected, for instance the location of a sun patch, or the treatment of heat conduction through a wall in one dimension only. Another drawback of TnrSys when performing short time step simulations of thick and highly insulated walls is its reliance on the Conduction Transfer Function method. Such problems have previously been reported by other authors (Flory-Celini, 2008; Delcroix et al., 2011; Savoyat et al., 2011).
As a thermal model of a building envelope should take into account rapid environmental variations, we have decided to develop a new transient thermal model that provides a faithful description heat transfer through walls in 3D over a short timescale. This numerical three dimensional transient thermal model is introduced in the following section of this paper. In order to evaluate the importance of the novel features and the critical parameters of the model (control volume size, sampling rate, and sun patch simulation), the model was systematically compared to contemporary models under a range of simulation configurations.

MODEL DEVELOPMENT

The building envelope is modeled following a three dimensional approach. The model represents a single room with a large window. The thermal behavior to be included in the model is summarized as follows:

– Solar radiation exchange (short-wave and long wave) with the sun patch and the radiation distribution
– Three-dimensional heat conduction
– Enthalpy of a single air node
– Convection between wall surfaces, the external and internal environment.

The walls of the model are simulated as a finite element mesh. Optimization of the meshing through the wall and its surfaces is described in a following section. Note that the model considers a single air node.

For each control volume, its temperature T is given by the partial differential heat conduction equation in three dimensions, coupled to the sum of convective and radiative exchange Φ_{TOT}:

$$CV\frac{\partial T}{\partial t} = \lambda_x\left(\frac{\partial T}{\partial x}\right)_{x+\frac{dx}{2}} dydz - \lambda_x\left(\frac{\partial T}{\partial x}\right)_{x-\frac{dx}{2}} dydz + \lambda_y\left(\frac{\partial T}{\partial y}\right)_{y+\frac{dy}{2}} dxdz - \lambda_y\left(\frac{\partial T}{\partial y}\right)_{y-\frac{dy}{2}} dxdz + \lambda_z\left(\frac{\partial T}{\partial z}\right)_{z+\frac{dz}{2}} dxdy - \lambda_z\left(\frac{\partial T}{\partial z}\right)_{z-\frac{dz}{2}} dxdy + \Phi_{\mathrm{TOT}} \quad (1)$$

where

$$\Phi_{\mathrm{TOT}} = \Phi_{\mathrm{SW}} + \Phi_{\mathrm{LW}} + \Phi_{\mathrm{CONV}} \quad (2)$$

and Φ_{CONV} is the convective heat flow between the surface and its environment and Φ_{LW} and Φ_{SW} are the long wave and short wave radiation. Thermal conductivities in the three directions are designated λ_x=λ_y= λ_z[W/mK] and the volumetric heat capacity is denoted by C [J/m^{3}K].

The energy balance equation for the air in the room with temperature T_{ai} is:

$$\rho \mathrm{C}_{air} V_c \frac{\partial Tai}{\partial t} = \sum_{n=0}^{N} Q\mathrm{C}_{air}(T_{ae} - T_{ai}) + \sum_{j=1}^{NM} Sh_{ci}(T_{SI} - T_{ai}) \quad (3)$$

Here T_{ae} is the exterior dry bulb temperature (°C), Q is the air flow (kg/s),C_{air} the heat capacity of the air (J/kgK), ρ the air density (kg/m^3), V_c the volume of the room, T_{SI} the interior surface temperature and h_{ci} the convective transfer coefficient. NM is the number of radiation balance equations corresponding to the number of surface mesh elements and N the number of zones (here N =1).

Short wave radiation

The total short wave radiation absorbed by the surfaces of a control volume is given by the vector the vector:

$$\{\Phi_{\mathrm{SWI}}\} = [S][a_{SWI}]\{E_{SW}\} \quad (4)$$

where $[S]$ is the surfaces matrix and $[a_{SWI}]$ is the matrix of absorptivities of the control volumes of the internal wall for the short wave radiation. $\{E_{SW}\}$ is the vector of radiation received by the mesh elements, obtained by resolving:

$$[S]\{E_{SW}\} = [S]\{E^{\circ}_{SW}\} + [S][\rho][FF]\{E_{SW}\} \quad (5)$$

Where $[\rho]$ is the reflectivity matrix. The view factors of the matrix $[FF]$ are calculated following the Nusselt analog (unit hemisphere). $\{E^{\circ}_{SW}\}$ is the vector composed by primary radiation received by the control volumes. It results from the horizontal beam radiation G_b and the diffuse radiation G_d received by the mesh elements:

$E^{\circ}_{SW,i} = \tau_b G_b R_b + \tau_d G_d R_d$, if the element i is in the sun patch, and (6)

$E^{\circ}_{SW,i} = \tau_d G_d R_d$ if the element i is not included in the sun patch

τ_b and τ_d are the direct and diffuse transmission coefficients of the glass and depend on the incidence angle of the beam, whereas $R_b = cos(\theta)/cos(\theta z)$ and $R_d = (1 + cos(p))/2$ provide direct and diffuse radiation components on a titled surface with slope p (Esveev and Kudish, 2008)(Liu et *al.*, 1969).

The sun patch position has been calculated by a geometrical test: the boundary of the window is projected on an orthogonal plane to the beam. The control volumes of the walls are projected on the same plane, and thus those projected cells belonging to the projection of the window are identified.

The short wave radiation received by the control volumes of external walls are determined depending on the position of the walls relative to the sun according to:

$$\{\Phi_{\mathrm{SWE}}\} = [S][a_{SWE}]\{G_b R_b + G_d R_d + (G_d + G_b)R_r\} \quad (7)$$

With $R_r = (1 - cos(p))alb/2$, and alb the ground albedo, which is the outside reflectivity of the ground.

Long wave radiation

Long wave radiation of the control volumes or the cells in the room of temperatures $\{T_{SI}\}$ are given by:

$$\{\Phi_{\mathrm{LWI}}\} = [a_{LWI}][S]\sigma\{{T_{SI}}^4 - T_m^4\} \quad (8)$$

which is linearized to:

$$\{\Phi_{\mathrm{LWI}}\} = [\varepsilon][S]\left[[I]\left[[I] - [FF][\rho]\right]^{-1}[FF][\varepsilon]\right]HR\{T_{SI} - T_m\} \quad (9)$$

where $[I]$ is the unit matrix, $[FF]$ the view factor matrix and $[\varepsilon]$ emissivity matrix of the cells in the wall. The radiation coefficients HR were fixed to 5.8 W/m²K.

Radiative heat transfer between external walls and the sky with effective temperature T_{sky}, and with the ground with temperature T_{earth} is given by:

$$\{\Phi_{\mathrm{LWE}}\} = h_{rs}[S]\left(\frac{1 + cos\, p}{2}\right)\left(\{T_{sky}\} - \{T_{SE}\}\right) + h_{re}[S]\left(\frac{1 - cos\, p}{2}\right)\left(\{T_{earth}\} - \{T_{SE}\}\right) \quad (10)$$

where $h_{rs} = h_{re}$ are the radiative coefficients with the ground and the sky. These were also fixed to 5.8 W/m²K.

Convective heat transfer

Convective heat flows between the environment and the external surface of the walls are given by:

$$\Phi_{CONV} = h_{ce}[S]\{Tae - T_{SE}\} \quad (11)$$

where $h_{ce} = 21$ W/m²K is the external convective coefficient.
The convective heat flux with the internal environment is:

$$\Phi_{CONV} = h_{ci}[S]\{Tai - T_{SI}\} \quad (12)$$

where the internal convective coefficient was assumed to be $h_{ci} = 8$ W/m²K

General resolution of the model

The input data are the building characteristics and the meteorological measurements. The numerical mesh of the room is generated with HEAT3 in cartesian coordinates (Blomberg, 1996).
Differential equations 1 and 2 are solved with a function of Matlab (ode23t). This function solves moderately stiff ordinary differential equations using the trapezoidal rule or Runge Kutta. This method is interesting because it solves the equations with an adapted and variable time-step. For fluctuant input data this method would automatically shorten the time step; similarly it would expand the time for periods with little fluctuation.

SIMULATIONS AND DISCUSSIONS

For all the simulations the same room dimensions were used: 3.01 m in width, 3.16 m in depth and 3.36 m in height. The walls, the ceiling and the roof are made of 10 cm thick concrete (λ=2.7 W/mK) and the room has a 1 cm thick window located on the south-facing wall (λ=1 W/mK)). Air flow in the room was neglected for all the simulations. Convective and radiative transfer coefficients are kept constant throughout the simulations.

The absorptivity and emissivity coefficients of the window and walls are listed in the table below.

Table 1: absorptivity and reflexivity of the wall and window

a_{SWI} of the wall	1
a_{SWI} of the window	0.05
a_{SWE} of the wall	0.6
a_{SWE} of the window	0.05
a_{LWE}	0.9
E	0.9

Minute-wise weather data were used from the meteorological station of Vaulx-en-Velin, France (latitude: 45°46'43''N and longitude : 4°55'21''E, height 170m) (http://idmp.entpe.fr/vaulx/mesfr.htm).
As a proof of principle test, the first model comprised the simple case of one control volume per internal surface and all radiation projected on the ground.

The model was subsequently transformed to more detailed configurations. As a first step, the importance of the weather data sampling was assessed. Then, the influence of cell size was analyzed and optimized for this room. Finally, simulations were performed for a time-varying sun patch.

First model: simplified hypotheses

For the first simulation the simplest case of one cell per surface was considered, neglecting reflections inside the room.
A visualization of this simple model, seen from the outside, is shown below generated in HEAT3 (Figure 1).

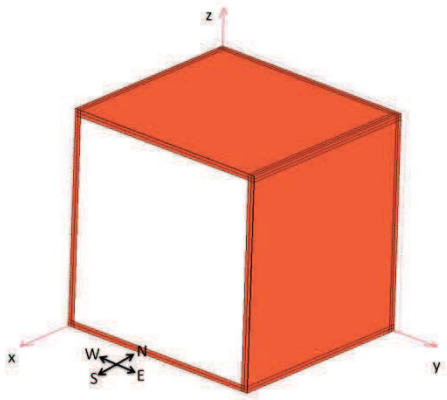

Figure 1: Shape and mesh of the room in HEAT3, the window appears in white

Each wall is described by only two cells. However, their connection to adjacent cells ensures that the heat transfer by conduction remains three dimensional.

For the same set of minute-wise weather data, the air temperature Tai predicted by the model was compared to that obtained to Dymola (Dymola Version 2013) and TRNSYS (TRNSYS Mathematical Reference, 1996) in order to verify consistency for this simplified arrangement (Figure 2).

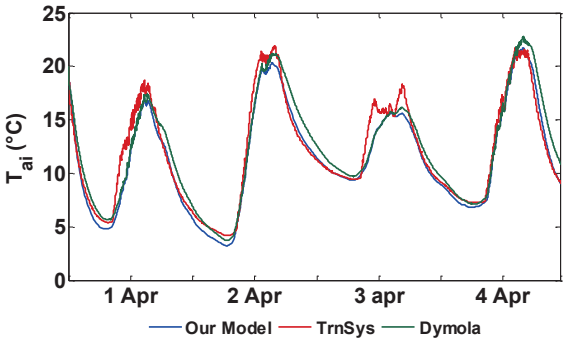

Figure 2: Comparison between TRNSYS - Dymola – our model

The small discrepancies observed may arise from slightly different calculations of short and long wave, the one dimensional approach employed by TRNSYS and Dymola, and the solver algorithms. Differences between 0 and 1°C degrees are observed between our

results and Dymola and differences between 0 and 2°C are observed between TrnSys and our model.

First model: sampling

Once we checked the general coherence of the model, we were interested in the sampling of weather data and its impact on the building simulation. Weather data are often taken at the time step of one hour. This time step may be sufficiently accurate if the aim is to study the overall behavior of a building during a year. It is poorly adapted however, to transient simulations designed to study the detailed thermal behavior of the envelope. To overcome this, Escudero (1989) modeled the perturbations as mathematical functions and applied Shannon's sampling theorem. He concluded that to represent outside bulb temperature variation in time a 40 min time step is enough, and a 5 and 2 min time step are enough for the diffuse and direct radiation.

For the first more detailed simulation, we chose to keep the radiation data at the time step of one minute, in order to keep the short-time solar variations. So, the model needs to solve the differential equations (1) and (2) for each sample of weather data. For the second simulation, a set of hourly data was generated by integrating minute-wise data in the previous hour. Simulation results using these aggregated data are shown superposed over those obtained with minute-wise measured weather data in Figure 3. The same number of cells was used for the two simulations. In red, we can see simulations using one minute time step measured weather data as an input of the model and in green, results with hourly input data.

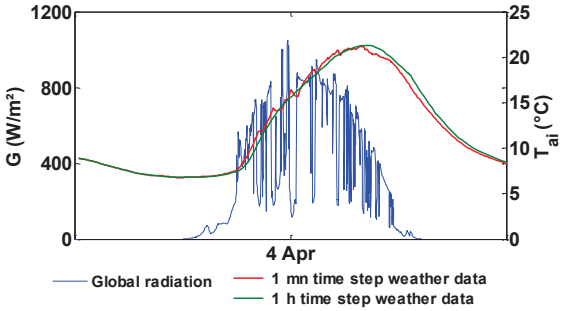

Figure 3: Impact of hourly and minute time-step weather data on the air temperature simulation

Short term variations in total radiation are clearly visible on the blue curve also shown in the figure. The weather fluctuations have an impact on the results simulated with the model for weather data with a time-step of one minute. Hourly data tend to smooth the fluctuations of the solar radiation and this has an impact on the building simulation results. Differences up to 1°C were observed on the air temperature calculation of the cell for the data sample.

Minute-wise data were retained for the following tests and simulations, in order to reveal any effects of these fluctuations on the numerical model. Note that this time step was not optimized. Indeed, a two or even three minute time step could be adequate.

First model: study of the spatial discretization

The importance of the cell size was first studied through the wall thickness. For a model, the greater the nodal discretization of the system, the finer the the calculated dynamics. Note that the time step of the thermal model and the narrowness of the spatial discretization of the described thermal system are interrelated.

When significant variations occur, for example fluctuations in solar radiation, the parts of the walls closest to the surfaces are the most affected. Considering the perturbations studied, the mesh resolution was enhanced in the edge regions in order to provide more detailed information near the surface next to these gains. So, it seems obvious to refine the cells next to the surfaces in contact with the room's volume. Figure 4 shows the interior air temperature of the room for 2,4,8 and 13 cells and with a fine meshing near the surface.

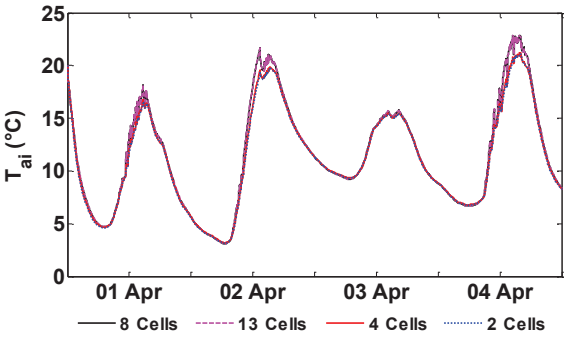

Figure 4: Air temperature for different spatial discretization

With few control volumes, fluctuations in air temperature are smooth. As the control volumes are thicker, the first volumes near the room absorb more of the solar variations by conduction.
The temperature differences, in green, vary from 0 to 2.3°C between a model with two and eight cells (Figure 5). These differences are largest when total incident solar radiation fluctuations are greatest. Indeed, we observe fewer differences for the third day, a day with less direct incident solar radiation.

For this wall thickness and with 13 cells, we observe very little difference with the model with eight cells. In conclusion, 8 cells seem adequate and will be kept in the wall for the following tests as it seems enough to absorb the perturbations. More cells would cause longer calculation times.

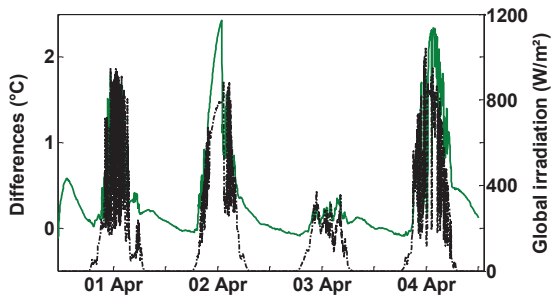

Figure 5: In black global incident solar radiation and in green the air temperature differences

For the same hypotheses, we compared the previous result (with a finer mesh through the thickness of the wall) and a simulation with a finer discretization of the wall surfaces (Figure 6). The red scattered line is the air temperature variation in time for one cell per surface but eight cells perpendicular to the wall.

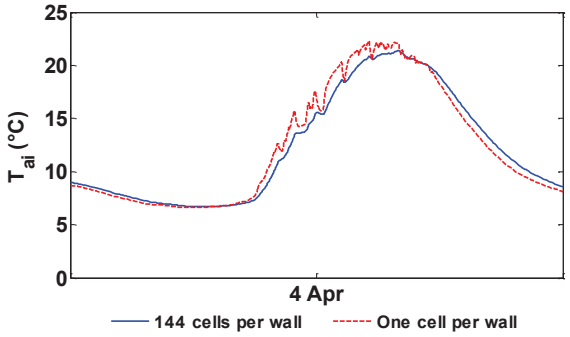

Figure 6: Influence of the spatial discretization of the walls' surfaces

In the figure, the blue line shows the results for a discretization of 144 cells per wall side and eight cells perpendicular to the wall. For this case, the three dimensional approach of the model has a greater influence on heat transfer. Thermal capacitance is more important as well as we observe that the response of air temperature to fluctuations in solar incident solar radiation. The air temperature differences between the two simulations are between 0 and 1.69 °C for the 4th April.

Second model: sun patch integration

Some of the gains which until now have been neglected are becoming more important in transient thermal modelling in low energy buildings (Duforestel et al., 2008). It is the case of fast variation of incident solar radiation and their distribution or what we call sun patch.

The incoming incident solar radiation in a room is projected as a sun patch. In most of the modeling approaches, the incoming incident solar radiation is constantly projected on the floor. Other hypotheses are to project only 60% of the incident solar radiation on the floor.

However Wall (1997) shows that it is important to consider the sun patch distribution, especially for heating requirements of glazed spaces.
Tittelein (2008) determines the sun position and projects the sun patch on the walls. He assigns to each wall a percentage of short wave radiation that varies in time. He shows that there is a difference of 8.5% for heating requirements between a model considering the sun patch and one without it. The next step now is to know whether assigning to each wall the same percentage of incident solar radiation is accurate enough. Indeed, a uniform distribution of solar heat flux on the walls seems adapted to one dimensional heat conduction; if we want to calculate accurately the impact of the perturbations it is important to locate the sun patch and therefore meshing the surfaces of the walls is necessary.

In order to locate the sun patch, the walls have been meshed in all the directions. In each direction we have 28 cells, 8 in each the wall's thickness and 12 on the surfaces. Internal reflections are integrated thanks to the view factors and absorptivity of the walls was fixed to 0.6 and reflexivity to 0.4. Finally, a three dimensional approach would be the best to do if we want to couple the sun patch movement and a transient thermal model. A better localization of the sun patch enables to locate overheating and the creation of plumes. These temperature differences will modify mean radiant temperature which is a comfort criterion.

The position of the sun patch depends on the position of the sun and the orientation of the building. On the figure below we show three moments in the day (morning, midday and afternoon) with the sun patch location (Figure 7 and 8). We have represented the cells located in the inside of the room. In black, no sun patch touches the cells of the walls, in gray it is the window and in white we show the cells touched by the sun patch. Note that the gray cells represent the window and it is oriented south.

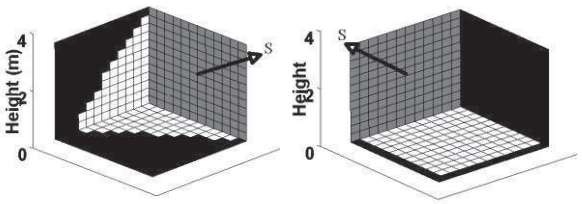

Figure 7: Sun patch location for the 4th April: morning and midday

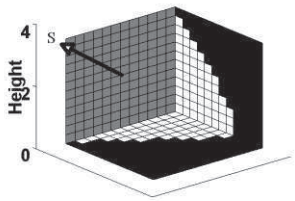

Figure 8: Sun patch location in the afternoon

We can see that for a simulation in April, the sun patch touches partially the floor, the wall oriented east and the one oriented west.

At 14h48 UTC on the 4th April, we have the inside temperature distribution shown on Figure 9.At this moment of the day, the sun patch is mainly on the floor and on the wall oriented east.The sun patch is clearly located, because the cells receiving important short wave radiation reach 22°C. Reflections are observed on the adjacent cells. Temperature differences between one cell and another cell can reach 8.8°C. Besides, the impact of the solar sun patch inside the room has an important effect on heat conduction transfer inside the walls.For the same simulated day and time we looked at the cross-section of two walls by fixing a height (Figure 10). At this moment the air of the cell is at 18.54°C and the outside temperature is of 13.4°C. We can observe that the cells of the first figure (Figure 10), which are never in the sun patch, are quite homogenous in temperature. On the second figure we can see that at the left hand side we have high temperatures, which are located in the sun patch. There is clearly a temperature gradient, and the magnitude of the gradient rises towards the sun patch.

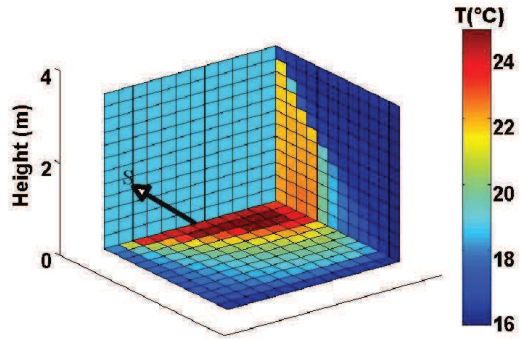

Figure 9: Inside temperature distribution of the floor, window and the wall oriented east at 14h48 UTC

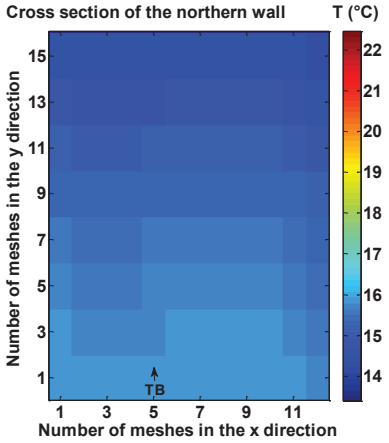

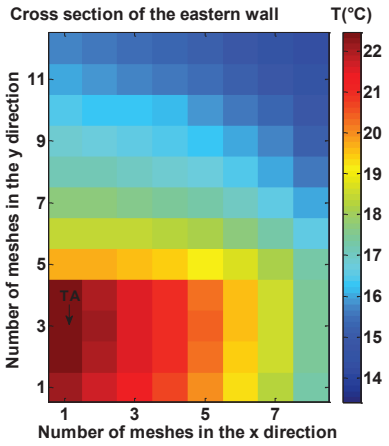

Figure 10: Horizontal cross-section of the cells and their temperature (height = 0.35cm)

This 3D heat transfer model compared to a simpler model is more discretized and a cell can be touched during a certain time by the sun patch, but at another moment it will be receiving only reflections or only diffuse radiation coming from other surfaces. We studied the temperature variation in time of cell TA and TB shown on figure 11. The red dotted line represents the temperatures of the cell TA and the unbroken blue line is the temperature of the cell TB. Cell TB is never receiving direct solar radiation during this day but in the morning it will be hotter than the cell TA as it is located nearer to the sun patch at this moment. In the afternoon, when the sun patch is located on the opposite side, cell TA is warmer. Temperature differences for these two cells during one day are between 0 and 4.6°C. The room's air temperature (black scattered line) depends on all the surrounding cells' temperatures and therefore is located in between of the other curves.

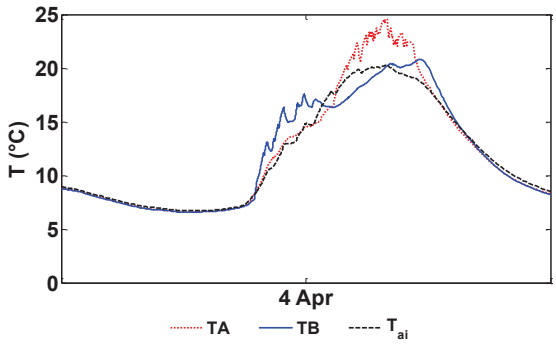

Figure 11: Temperature of cell TA and TB and the temperature of the room's air

The heating of some areas of the wall due to the sun patch changes the transferred conduction fluxes to the outside. This is observed on the external surfaces where higher temperatures are observed where the nearby meshed volumes were touched by the sun patch (Figure 12) located on the inside of the eastern wall (Figure 9).

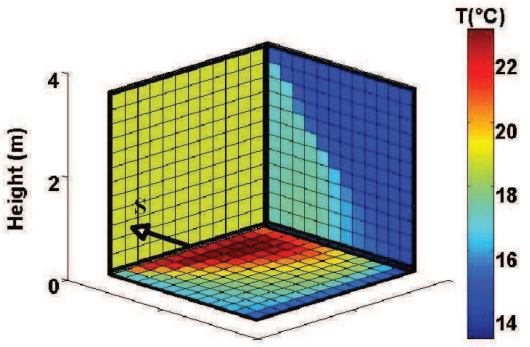

Figure 12: Outside temperature distribution of the floor, window and the wall oriented east at 14h48 UTC on the 4th April

We have compared the results from the first study done with a constant projection of the short wave radiation on the floor to this study with the sun patch model. In blue, we can see the room's air temperature when we project all the incident solar radiation on the floor with the same absorptivity and reflectivity than for the sun patch model. The black dotted line is the air temperature variation in time after integrating the sun patch. When integrating the sun patch we have the same incoming radiation through the window than with no sun patch, but the spatial distribution of the radiation touching the walls and control volumes are different. With the sun patch we have fewer cells touched by the direct radiation than when projecting the radiation on the floor. Therefore with the sun patch model, we tend to have higher temperatures for the cells touched by the sun patch but we have a smaller area than when supposing that the radiation touches the whole floor's surface. In average, with the sun patch model we have temperature differences between the surfaces and the air which are smaller than with the other model. That is the reason why, the air temperature T_{ai} has a smaller gradient when we add the sun patch (Figure 13). Over all, we obtain a less fluctuant temperature variation with the sun patch integration, than with the simple case. Differences between 0 – 1.09°C are observed.

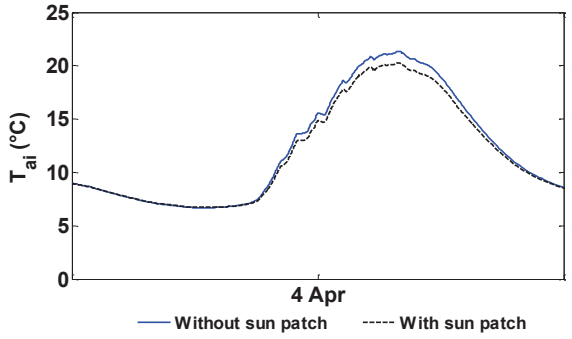

Figure 13: Air temperature of the cell for two simulations: with and without sun patch

CONCLUSION

We have started with a simplified model and with current taken hypotheses: few cells, all the short wave radiation on the floor and hourly weather data. We have gradually transformed this model in a more complex model, by working on the sampling rate, the spatial discretization and the sun patch simulation.
In conclusion, taking hourly weather data can lead to smoothing too much the solar radiation fluctuations and it has an impact on the simulated results.
A minimum number of cells were necessary to model in three dimensions the heat transfers if we want to use short time steps. By adding the sun patch position moving in time, we have observed differences concerning the surfaces temperature distribution, the incident short wave length radiation calculation and therefore differences of the air of the room have been observed. In conclusion, if a detailed envelope model is required in the building area, using a 3D model and considering the rapid weather variations in time with the sun patch leads to important improvements, which have been quantified.

FUTURE WORK

These results have to be validated with experimental data, and therefore we are working on an in situ experimental set up.

ACKNOLEDGEMENTS

This work has been supported by the French National Agency for Research (ANR), in the framework of the project "SUPERBAT", ANR-10-HABISOL-004-06.
I would also like to thank Leon Gaillard and Pierrick Haurant for their contributions.

REFERENCES

ADEME, Stratégie utilisation rationnelle de l'énergie, 2005. Chapitre II : « Les bâtiments », page 1, www2.ademe.fr

Blomberg, 1996. HEAT CONDUCTION IN TWO AND THREE DIMENSIONS Computer Modelling of Building Physics Applications.

CODYBA www.jnlog.com/codyba1.htm

B. Delcroix, M. Kummert, A. Daoud, and M. Hiller, « Conduction Transfer Functions in TRNSYS multizone building model: Current implementation, limitations and possible improvements », Fifth National Conference of IBPSA-USA, Madison, Wisconsin, August 2012.

Duforestel T., Bouia, H., Hartmann, O., Roux, J.J., Krauss, G., 2008. Les outils de modélisation énergétique des bâtiments très basse consommation.

Dymola Version 2013, (10.01.2013) homepage: http://www.3ds.com/products/catia/portfolio/dymola

Escudero Alain, 1989. Etude du comportement thermique des bâtiments. Proposition d'un modèle a deux dynamiques. PhD INSA de Lyon

Esveev, E.G. and Kudish, A.I., 2009. The assessment of different models to predict the global solar radiation on a surface tilted to the south. Solar Energy 83 377–388

International Daylight Measurement Programme, Station de l'ENTPE de Vaulx-en-Velin, http://idmp.entpe.fr/vaulx/stafr.htm

Flory-Celini C., 'Modélisation et positionnement de solutions bioclimatiques dans le bâtiment résidentiel existant', PhD, Université Claude Bernard Lyon 1, 2008

Liu, B.Y.H., Jordan, R.C., 1961. Daily insolation on surfaces tilted towards to equator. Trans ASHRAE 67, 526–541.

Savoyat J., Johannes K., Virgone J., 2011.Integration of thick wall in TRNSYS simulation. ISES solar world congress, Kassel, Germany, 2011

Tittelein, 2008. Environnements de simulation adaptés à l'étude du comportement énergétique des bâtiments basse consommation. Doctorat Université de Savoie

TRNSYS Mathematical Reference, 1996. Solar Energy Laboratory Madison, United States, University of Wisconsin.

Wall, 1997. Distribution of solar radiation in glazed spaces and adjacent buildings. A comparison of simulation programs. Energy and Buildings 26, 129-13